Intermetallics 92 (2018) 119–125

Contents lists available at ScienceDirect

Intermetallics

journal homepage: www.elsevier.com/locate/intermet

Thermal conductivity of $Ni_3(Si,Ti)$ single-phase alloys

Satoshi Semboshi[a,b,*], Tatsuro Takeuchi[b], Yasuyuki Kaneno[b], Akihiro Iwase[b], Takayuki Takasugi[b]

[a] Institute for Materials Research, Tohoku University, Katahira 2-1-1, Aoba-ku, Sendai, Miyagi 980-8577, Japan
[b] Department of Materials Science, Osaka Prefecture University, Gakuen-cho 1-1, Naka-ku, Sakai, Osaka 599-8531, Japan

ARTICLE INFO

Keywords:
A. Intermetallics ($Ni_3(Si, Ti)$ alloys)
B. Thermal properties
D. Microstructure
E. Physical properties

ABSTRACT

Thermal conductivities of $Ni_3(Si,Ti)$ single-phase alloys with an $L1_2$ structure as functions of composition and temperature were measured to provide information for high-temperature structural applications. It was confirmed that the $Ni_3(Si,Ti)$ alloy has an extremely large single-phase region for the compositions $Ni_{78}(Si_{22-x},Ti_x)$ (x = 0–12 at.%), $Ni_{89-y}(Si_{11},Ti_y)$ (y = 9.5–12 at.%), and $Ni_{89-z}(Si_z,Ti_{11})$ (z = 9.5–12 at.%). The thermal conductivities at 293 K of all the $Ni_3(Si,Ti)$ single-phase alloys were estimated to be between 8 W/mK and 12 W/mK, which are lower than those of almost all other stoichiometric compounds. In the $Ni_3(Si,Ti)$ single-phase region, the thermal conductivity increased more significantly by increasing the Ni content than by varying the Si and Ti contents. The thermal conductivity of all the $Ni_3(Si,Ti)$ single-phase alloys increased monotonically with an increase in temperature. The temperature coefficient of thermal conductivity increased as the value of the thermal conductivity at 293 K was low, according to Mooij's relationship. Consequently, the thermal conductivity in the $Ni_3(Si,Ti)$ single-phase region became larger and less sensitive to the composition at higher temperatures above 1073 K, ranging between 22 W/mK and 24 W/mK.

1. Introduction

Nickel-based intermetallic compounds, such as $L1_2$-type Ni_3Al [1–3], Ni_3Si [4], B2-type NiAl [5], and $D0_a$-type Ni_3Nb [6] based alloys, are attractive for high-temperature structural applications, because of their high mechanical strength at elevated temperatures. Among these alloys, those based on Ni_3Si have properties that are considered desirable for structural materials; they show increased strength with increasing temperature (i.e., anomalous temperature dependency of strength) [4,7], and excellent oxidation resistance. In particular, $L1_2$-type Ni_3Si alloys to which elemental Ti has been added, and which are denoted as $Ni_3(Si,Ti)$, are interesting from a practical viewpoint. This is because alloys with an off-stoichiometric composition of approximately Ni 78 at.%- Si 11 at.%- Si 11 at.% Ti can deform even in cold-rolling, unlike a number of intermetallic compounds [8,9]. Therefore, extensive investigations were conducted in an attempt to further enhance the mechanical properties of $Ni_3(Si,Ti)$ alloys and to understand their microstructural and compositional features [10–14]. On the contrary, to obtain the reliability required for high-temperature structural products, the thermal conductivity should also be an important criterion when selecting an appropriate material, although measurements of the thermal conductivity of $Ni_3(Si,Ti)$ single-phase alloys have been limited to determining the stoichiometric composition of Ni_3Ti with a $D0_{24}$ structure [15]. In this study, we measured the thermal conductivity of $Ni_3(Si,Ti)$ single-phase alloys in the temperature range between 293 K and 1073 K, in which the alloys are intended for high-temperature structural applications. The effects of the composition and temperature on the thermal conductivity of the alloys are also discussed.

2. Experimental

As shown in the Ni-Si-Ti ternary phase diagram in Fig. 1 [8], the $L1_2$-type $Ni_3(Si,Ti)$ phase has an extremely large mutual solid solution range along a pseudo-binary line between Ni_3Si with an $L1_2$ structure and Ni_3Ti with a $D0_{24}$ structure, and also a certain width of non-stoichiometry in the Ni-rich region. Based on Fig. 1, 12 button ingots of $Ni_3(Si,Ti)$ single-phase alloys were fabricated by arc-melting in an argon atmosphere using 99.99 wt.% nickel, 99.99 wt.% silicon, and 99.9 wt.% titanium tips as raw materials. Each button was inverted and then melted at least four times in order to ensure homogeneity. Table 1 lists the nominal and chemically analyzed compositions of the buttons prepared in this study, and indicates that the difference between them is insignificant. These alloys are hereafter denoted by their nominal composition in at.%; for example, alloys with a nominal composition of Ni 78 at.%-Si 20 at.%-Ti 2 at.% are presented as $Ni_{78}(Si_{20},Ti_2)$. The alloys were homogenized at 1323 K for 48 h under vacuum and then cooled in a furnace. Thereafter, the alloy buttons were cut into disk-shaped specimens measuring 10 mm in diameter and 1.5 mm in

* Corresponding author. Institute for Materials Research, Tohoku University, Katahira 2-1-1, Aoba-ku, Sendai, Miyagi 980-8577, Japan.
E-mail address: semboshi@imr.tohoku.ac.jp (S. Semboshi).

http://dx.doi.org/10.1016/j.intermet.2017.10.002
Received 4 September 2017; Received in revised form 1 October 2017; Accepted 6 October 2017
Available online 12 October 2017
0966-9795/

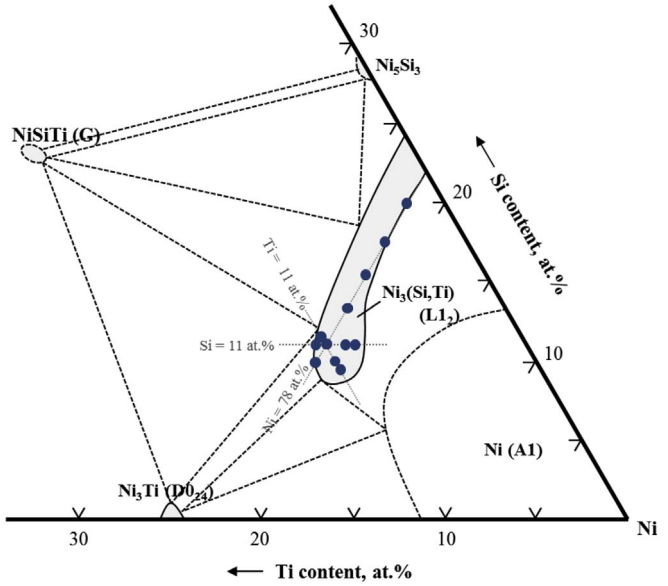

Fig. 1. Nickel-corner of the Ni-Si-Ti ternary phase diagram at 1173 K [8]. Solid circles in the $Ni_3(Si,Ti)$ single-phase region show the alloy composition prepared in this study.

Table 1
Nominal and chemical compositions of the alloys used in this study.

Specimen		Ni/at.%	Si/at.%	Ti/at.%
$Ni_{78}(Si_{22-x}, Ti_x)$	$Ni_{78}(Si_{20},Ti_2)$	78.5	19.4	2.1
	$Ni_{78}(Si_{17},Ti_5)$	78.5	17	4.5
	$Ni_{78}(Si_{16},Ti_6)$	78.0	15.6	6.4
	$Ni_{78}(Si_{13},Ti_9)$	78.4	12.8	8.8
	$Ni_{78}(Si_{11},Ti_{11})$	78.0	11.2	10.9
	$Ni_{78}(Si_9,Ti_{13})$	77.5	9.3	13.2
$Ni_{89-y}(Si_{11}, Ti_y)$	$Ni_{79.5}(Si_{11},Ti_{9.5})$	79.9	10.6	9.5
	$Ni_{79}(Si_{11},Ti_{10})$	79.5	10.5	10.0
	$Ni_{78}(Si_{11},Ti_{11})$	78.0	11.2	10.9
	$Ni_{77}(Si_{11}Ti_{12})$	77.3	10.6	12.1
$Ni_{89-z}(Si_z, Ti_{11})$	$Ni_{79.5}(Si_{9.5},Ti_{11})$	79.9	9.2	10.9
	$Ni_{79}(Si_{10},Ti_{11})$	78.9	10.0	11.1
	$Ni_{78}(Si_{11},Ti_{11})$	78.0	11.2	10.9
	$Ni_{77}(Si_{12}Ti_{11})$	77.5	11.8	10.7

thickness via electrical-discharge machining.

The microstructures of the specimens were observed with a field emission scanning electron microscope (FESEM; SM-7000F, JEOL) operating at 15 kV. For the FESEM-based microstructural observations, each disk-shaped specimen was mechanically polished using 2000-grade emery paper and then electrochemically polished with a solution of 15 vol.% sulfuric acid and 85 vol.% methanol at 258 K under an applied DC voltage of 15 V for 20 s. The structure of the prepared alloys was analyzed by X-ray diffraction (XRD) using a PANalytical X'pert Pro diffractometer with CuKα radiation (wavelength, λ = 0.1542 nm) in the Bragg-Brentano geometry. The lattice parameter of the $Ni_3(Si,Ti)$ phase was determined by extrapolating the lattice parameters measured from the five reflections 111, 200, 210, 220, and 311 to $2\theta = 90^\circ$ as a function of $\cos^2\theta$. The thermal conductivity, λ, of the disk-shaped specimens was measured by the laser-flash method at temperatures between 293 K and 1073 K using an ULVAC-RIKO TC-8000 instrument. Details of the mechanism of these measurements were described elsewhere [16–18]. The electrical conductivity λ^e $[(\Omega m)^{-1}]$ of the disk-shaped specimens was measured by way of an eddy-current method using a SIGMATEST 2.069, FOERSTER meter [19]. The λ^e value was converted into thermal conductivity λ using the Wiedemann-Franz law [20,21], as given by the following equation,

$$\lambda = AL_o T\lambda^e + B \quad (1)$$

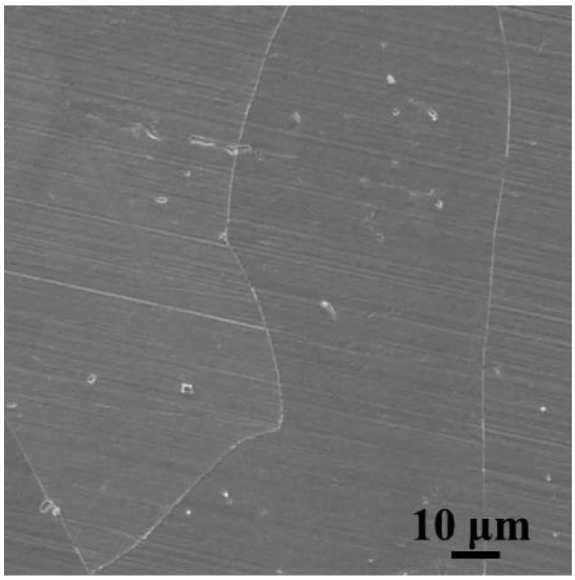

Fig. 2. FESEM micrograph of the $Ni_{78}(Si_{11},Ti_{11})$ alloy.

where L_0 is the Lorenz number ($L_0 = 2.45 \times 10^{-8}$ WΩ/K^2), T is the absolute temperature [K], and A and B are constants that are adjusted to fit the data. In the case of a Ni-based alloy, A and B have been reported to be 0.869 and 8.4 W/mK, respectively [20], which were adopted in this study.

3. Results

3.1. Microstructure

Fig. 2 shows the FESEM micrograph for the $Ni_{78}(Si_{11},Ti_{11})$ alloy. The microstructure of the $Ni_{78}(Si_{11},Ti_{11})$ alloy exhibited a single phase with a grain size of several hundred micrometers. Fig. 3 shows the XRD profile for the $Ni_{78}(Si_{11},Ti_{11})$ alloy, in which all the peaks were indexed by an $L1_2$ structure (Space group: $Pm3()m$, lattice parameter: a = 0.3550 nm). Therefore, it was confirmed that the $Ni_{78}(Si_{11},Ti_{11})$ alloy has a $Ni_3(Si,Ti)$ single phase. Similarly, it was confirmed that the other alloys prepared in this study were also constituent of a $Ni_3(Si,Ti)$ single phase. The result is consistent with the Ni-Si-Ti ternary phase diagram shown in Fig. 1.

Fig. 4 shows the variation of the lattice parameter of the $Ni_3(Si,Ti)$

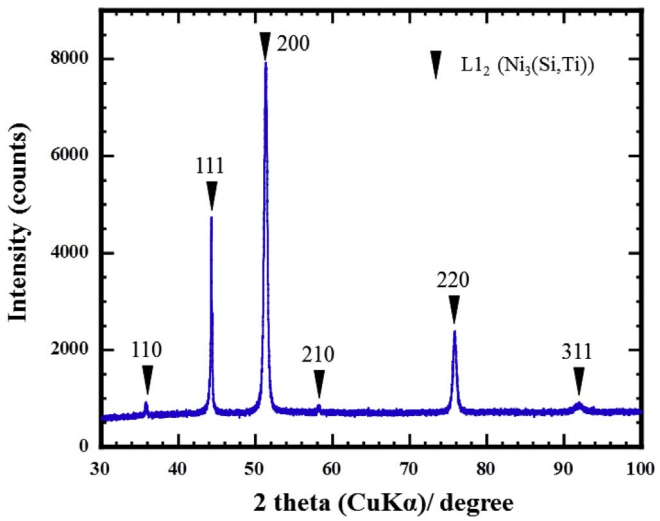

Fig. 3. X-ray diffraction profile of the $Ni_{78}(Si_{11},Ti_{11})$ alloy.

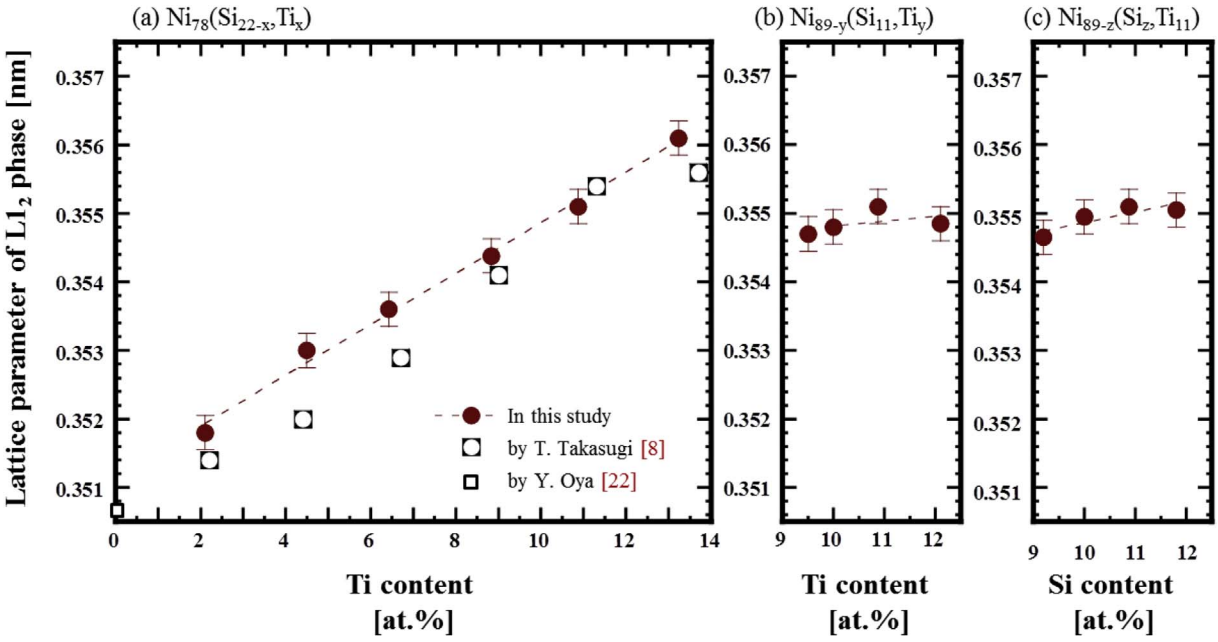

Fig. 4. Variations of the lattice parameters of the (a) $Ni_{78}(Si_{22-x},Ti_x)$, (b) $Ni_{89-y}(Si_{11},Ti_y)$, and (c) $Ni_{89-z}(Si_z,Ti_{11})$ alloys with the elemental content, together with the data by Takasugi et al. and Oya et al. [8,22].

phase as a function of the composition of the alloy, together with the data by Takasugi et al. [8] and Oya et al. [22]. The lattice parameters of the $Ni_3(Si,Ti)$ phase with a constant Ni content of 78 at.%, denoted as $Ni_{78}(Si_{22-x},Ti_x)$, increased linearly with increasing Ti content, x, which is in good agreement with the previous report by Takasugi et al. [8]. This indicates that the $Ni_3(Si,Ti)$ lattice expands when Si atoms are replaced with Ti atoms, and supports the aforementioned finding that the specimens are composed of a compositionally continuous $Ni_3(Si,Ti)$ single phase. The increase in the lattice parameter of the $Ni_3(Si,Ti)$ phase with increasing Ti content can also be explained by the term of Vegard's law in the case of solid solution phases; the Goldschmidt atomic radii of Ni, Si, and Ti are 0.124 nm, 0.124 nm, and 0.132 nm, respectively. Therefore, the replacement of Si with Ti in the $Ni_{78}(Si_{22-x},Ti_x)$ alloys would reasonably be expected to result in the expansion of the $L1_2$ lattice as shown in Fig. 4(a). The lattice parameters of the specimens with a constant Si or Ti content of 11 at.%, shown in Fig. 4(b) and (c), respectively, either seem to be the same or to increase slightly with increasing Ti or Si content, although the variation occurred within the experimental accuracy. Taking into account the Goldschmidt atomic radii abovementioned, replacement of Ni atoms by Ti atom in $Ni_{89-y}(Si_{11},Ti_y)$ alloys (Fig. 4(b)) should cause a similar increase with the case of the $Ni_{78}(Si_{22-x},Ti_x)$ alloys shown in Fig. 4(a), whereas replacement of Ni atoms by Si atoms should not change in lattice parameter. The discrepancy between prediction and experimental results must be because the compositional range of y and z was not wide enough to detect the change in lattice parameter clearly.

3.2. Thermal conductivity

Fig. 5 shows the thermal conductivity at 293 K, λ_{293}, for the $Ni_3(Si,Ti)$ single-phase specimens, together with the data converted from the electrical conductivity, λ_{293}^e, using eq. (1). The values of λ_{293} measured by the laser-flash method agreed well with those of λ_{293}^e, although the former values were always slightly lower than the latter. The λ_{293} of the $Ni_3(Si,Ti)$ single-phase alloy specimens prepared in this study range between 8.5 and 11 W/mK, which, according to expectation, are lower than that of Ni_3Al (28 W/mK), Ni_3Ga (27 W/mK), and Ni_3Ge (25 W/mK) in $L1_2$ stoichiometric compounds, and Ni_3Ti (30 W/mK) in $D0_{24}$ [15,23–25].

The λ_{293} of the $Ni_{78}(Si_{22-x},Ti_x)$ specimens decreases gradually with increasing Ti content, x, as shown in Fig. 5(a). The λ_{293} of the $Ni_{89-y}(Si_{11},Ti_y)$ and $Ni_{89-z}(Si_z,Ti_{11})$ specimens also decrease with increasing Ti and Si content, respectively, and these changes were more significant than in the case of the $Ni_{78}(Si_{22-x},Ti_x)$ specimens (see Fig. 5(b) and (c)). The decreasing of the λ_{293} per at.% of added element was approximately measured to be 0.12 W/mK·at.% for the $Ni_{78}(Si_{22-x},Ti_x)$ specimens, 0.89 W/mK·at.% for the $Ni_{89-y}(Si_{11},Ti_y)$ specimens, and 0.73 W/mK·at.% for the $Ni_{89-z}(Si_z,Ti_{11})$ specimens. These changes are relatively small in comparison with that of Ni_3Al to which a ternary element has been added; e.g., approximately 2.3 W/mK·at.% for the $Ni_{75}(Al_{25-x},Si_x)$ specimen, and 2.7 W/mK·at.% for the $Ni_{75}(Al_{25-x},Ti_x)$ specimen [23]. Thus, we can state that the λ_{293} of $Ni_3(Si,Ti)$ single-phase alloys shows less compositional sensitivity than the other $L1_2$ intermetallic compounds.

Fig. 6 shows the variation of the thermal conductivity of the $Ni_{78}(Si_{11},Ti_{11})$, $Ni_{78}(Si_{20},Ti_2)$, $Ni_{79.5}(Si_{11},Ti_{9.5})$, and $Ni_{79.5}(Si_{9.5},Ti_{11})$ alloys as a function of temperature. The thermal conductivity of all four specimens increased monotonically with temperature. A similar tendency was observed for the other specimens prepared in this study. The temperature coefficient of thermal conductivity, α, is defined by the following equation:

$$\alpha = \{(\lambda_{1073}-\lambda_{293})/(1073-293)\} /\lambda_{293} \ldots \quad (2)$$

where λ_{1073} is the thermal conductivity at 1073 K. Fig. 7 plots the value of the coefficient α of the $Ni_3(Si,Ti)$ single-phase specimens as a function of the elemental content. In the $Ni_3(Si,Ti)$ single-phase specimens, α increases as the values of x, y, and z increase.

The thermal conductivity at the high temperature of 1073 K, λ_{1073}, for the $Ni_3(Si,Ti)$ shingle-phase specimens is also plotted in Fig. 5. This reveals that the value of λ_{1073} was enhanced in comparison with that of λ_{293} in each specimen, because the coefficient α was always positive as shown in Fig. 7. The value of λ_{1073} varied with the elemental content in a manner similar to that of λ_{293}. The decreasing of the λ_{293} per at.% of added element was measured to be 0.11 W/mK·at.% for the $Ni_{78}(Si_{22-x},Ti_x)$ specimens, 0.85 W/mK·at.% for the $Ni_{89-y}(Si_{11},Ti_y)$ specimens, and 0.60 W/mK·at.% for the $Ni_{89-z}(Si_z,Ti_{11})$ specimens, which were the same or slightly less than the case of λ_{293}.

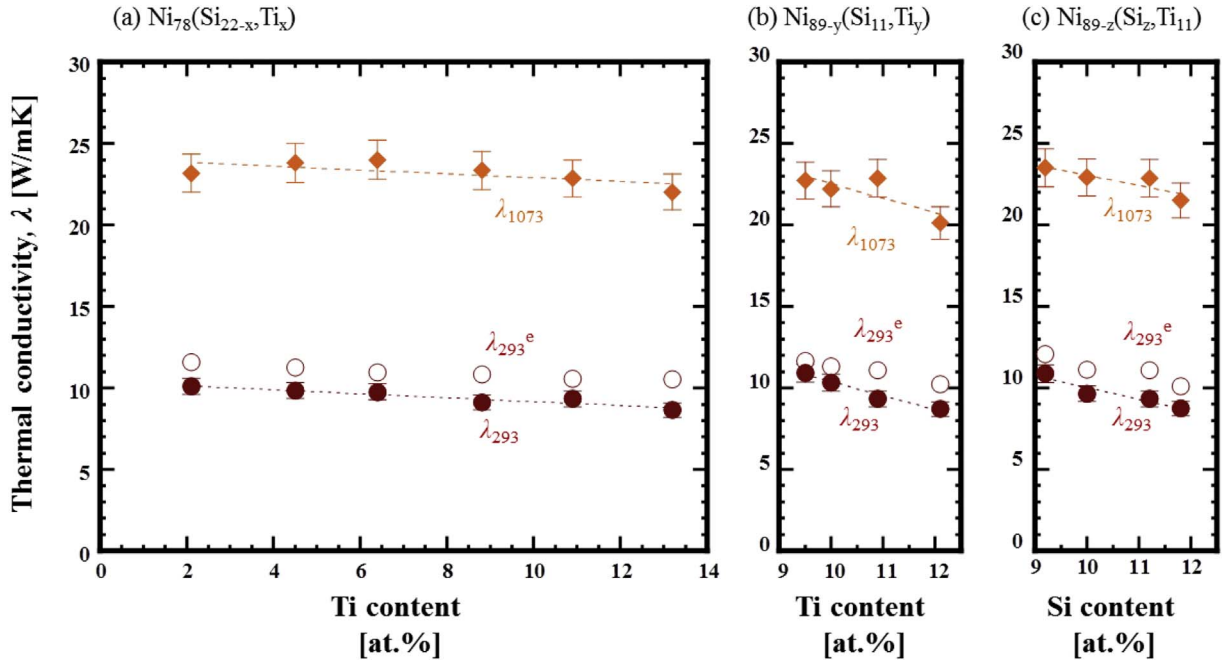

Fig. 5. Variations of the thermal conductivity at 293 K and 1073 K of the (a) $Ni_{78}(Si_{22-x},Ti_x)$, (b) $Ni_{89-y}(Si_{11},Ti_y)$, and (c) $Ni_{89-z}(Si_z,Ti_{11})$ alloys as a function of the elemental content. The thermal conductivity at 293 K, converted from the electrical conductivity measurements, was also plotted (open circles).

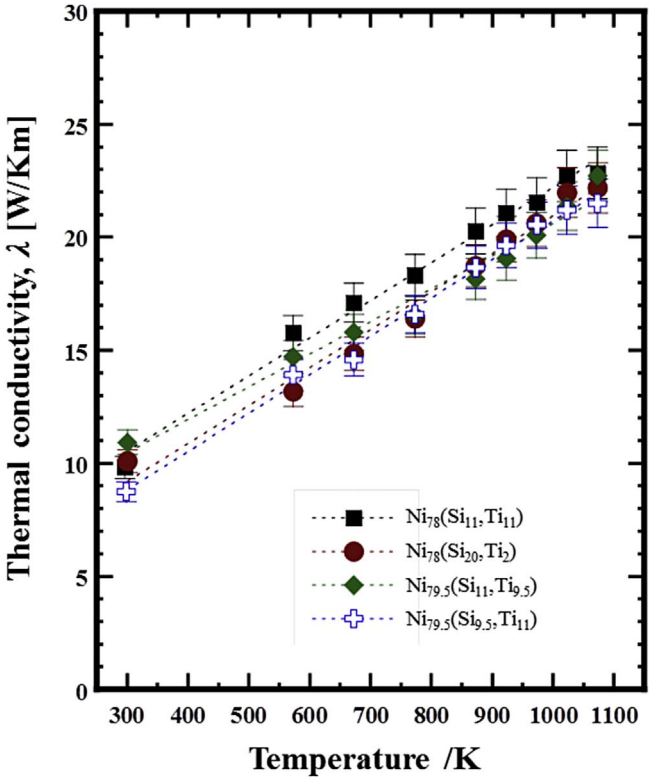

Fig. 6. Temperature dependence of the thermal conductivity of the $Ni_{78}(Si_{11},Ti_{11})$, $Ni_{78}(Si_{20},Ti_2)$, $Ni_{79.5}(Si_{11},Ti_{9.5})$, and $Ni_{79.5}(Si_{9.5},Ti_{11})$ alloys.

4. Discussion

4.1. Compositional dependency

In a metallic *A-B* binary alloy system with continuous solid solutions, the compositional dependence of the thermal conductivity can be estimated by Nordheim's relationship, which was originally proposed for electrical conductivity and resistivity [26,27]. The compositional dependence of the electrical conductivity λ^e and resistivity ρ^e is approximately expressed by the following equation:

$$1/\lambda^e = \rho^e = \rho_A{}^e + k' C_B(1-C_B) \ldots \quad (3)$$

where $\rho_A{}^e$ are the electrical resistivity of the pure metal of element *A*, C_B is the composition of additional solute element *B*, and *k'* is a constant that depends on the *A-B* alloy system. When the Wiedemann-Franz relation is available for the *A-B* alloy system, the thermal conductivity, λ, can be given as follows [20,21,25]:

$$1/\lambda = \rho = 1/\lambda_A + k\, C_B(1-C_B) \ldots \quad (4)$$

where ρ is the thermal resistivity, λ_A is the thermal conductivity of the pure metal of element *A*, and *k* is a constant that depends on the *A-B* alloy system.

It has been recognized that the relationship holds not only for solid solutions but also for intermetallic compounds [24,28]. Fig. 8 shows the plots for the inverse of λ (i.e., thermal resistivity, ρ) at 293 K and 1073 K as a function of the elemental content. The values of λ [W/mK] exhibited linear behavior against the elemental content of *x*, *y*, and *z*, and therefore could be fitted by the Nordheim equation given in eq. (4) as follows;

$Ni_{78}(Si_{22-x},Ti_x)$ at 293 K: $1/\lambda = 0.0952 + 0.0014\, x(1-x) \ldots$ (5)

$Ni_{89-y}(Si_{11},Ti_y)$ at 293 K: $1/\lambda = 0.0066 + 0.0090\, y(1-y) \ldots$ (6)

$Ni_{89-z}(Si_z,Ti_{11})$ at 293 K: $1/\lambda = 0.0231 + 0.0077\, z(1-z) \ldots$ (7)

$Ni_{78}(Si_{22-x},Ti_x)$ at 1073 K: $1/\lambda = 0.0414 + 0.0002\, x(1-x) \ldots$ (8)

$Ni_{89-y}(Si_{11},Ti_y)$ at 1073 K: $1/\lambda = 0.0248 + 0.0020\, y(1-y) \ldots$ (9)

$Ni_{89-z}(Si_z,Ti_{11})$ at 1073 K: $1/\lambda = 0.0309 + 0.0012\, z(1-z) \ldots$ (10)

The above measurements and equations enable us to draw an approximate contour map of the thermal conductivity at 293 K and 1073 K on the Ni-Si-Ti phase diagram, as shown in Fig. 9. The maps enable us to derive some notable features. For instance, both the thermal conductivities of λ_{293} and λ_{1073} in the $Ni_3(Si,Ti)$ single-phase specimens are more sensitive in terms of Ni content than Si and Ti

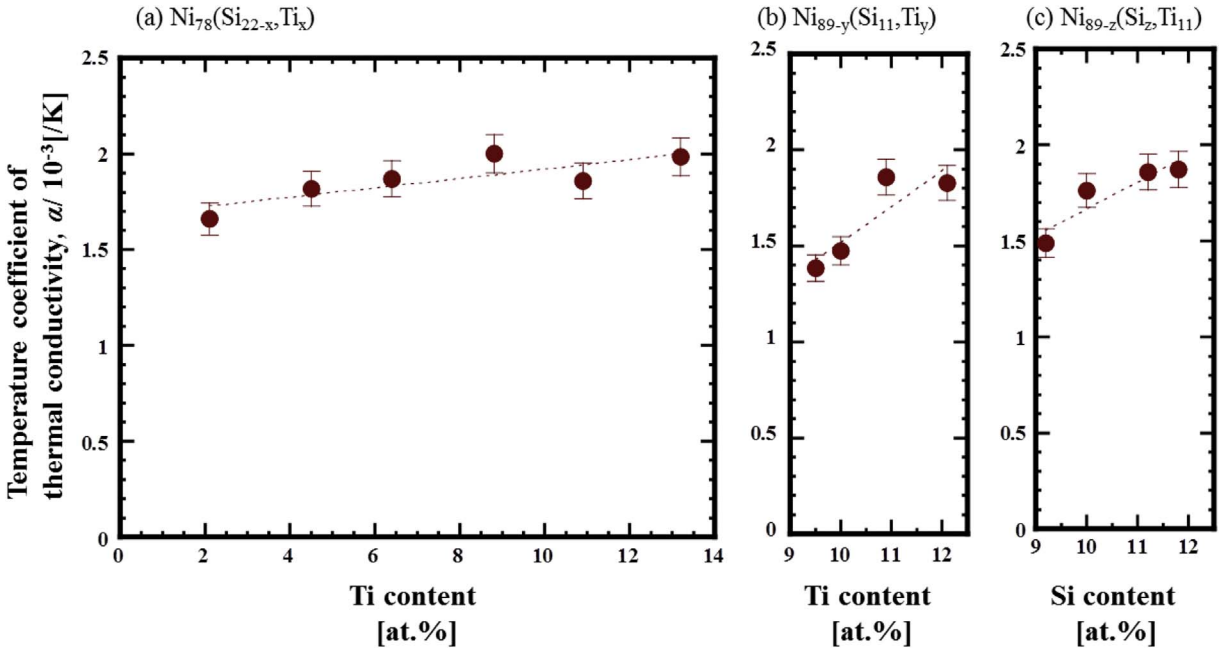

Fig. 7. Variations of the temperature coefficient of the (a) $Ni_{78}(Si_{22-x},Ti_x)$, (b) $Ni_{89-y}(Si_{11},Ti_y)$, and (c) $Ni_{89-z}(Si_z,Ti_{11})$ alloys as a function of the elemental content.

content. This suggests that λ_{293} and λ_{1073} would have a maximum value for the alloy with a maximum content of Ni in the $Ni_3(Si,Ti)$ single-phase specimens. The maximum value of the thermal conductivity is estimated to be 12 W/mK at 293 K and 24 W/mK at 1073 K for the $Ni_{91}(Si_{9.5},Ti_{9.5})$ alloys. The interval of the contour curves for the thermal conductivity should be wider at a high temperature (i.e., the compositional dependence for the thermal conductivity should become less sensitive at higher temperatures).

4.2. Temperature dependency

The temperature dependency of the thermal conductivity of ordered intermetallic compounds, together with the data for pure metals, Cu-Al solid solutions, Ni-based alloys, low and high alloy steels, and disordered fcc alloys with compositions of Pt_3Cu, Ni_3Zn, and Pt_3Ni, was summarized by Terada et al., and is shown in Fig. 10 [15,24]. Here, Terada et al. expressed the temperature coefficient of thermal conductivity, β, by the following equation:

$$\beta = (1/\lambda_{300})\{(\lambda_{1100} - \lambda_{300})/(1100 - 300)\} \ldots \quad (11)$$

As an overall tendency, the thermal conductivity at 300 K for metallic materials should be inversely correlated with the temperature coefficient, which is known as Mooij's relationship for the electrical resistivity for binary alloys [29,30]. Fig. 10 indicates that pure metals and low alloy steels have a high thermal conductivity at 300 K but a negative temperature coefficient, which means that the thermal conductivity decreases with increasing temperature. In contrast, high alloy

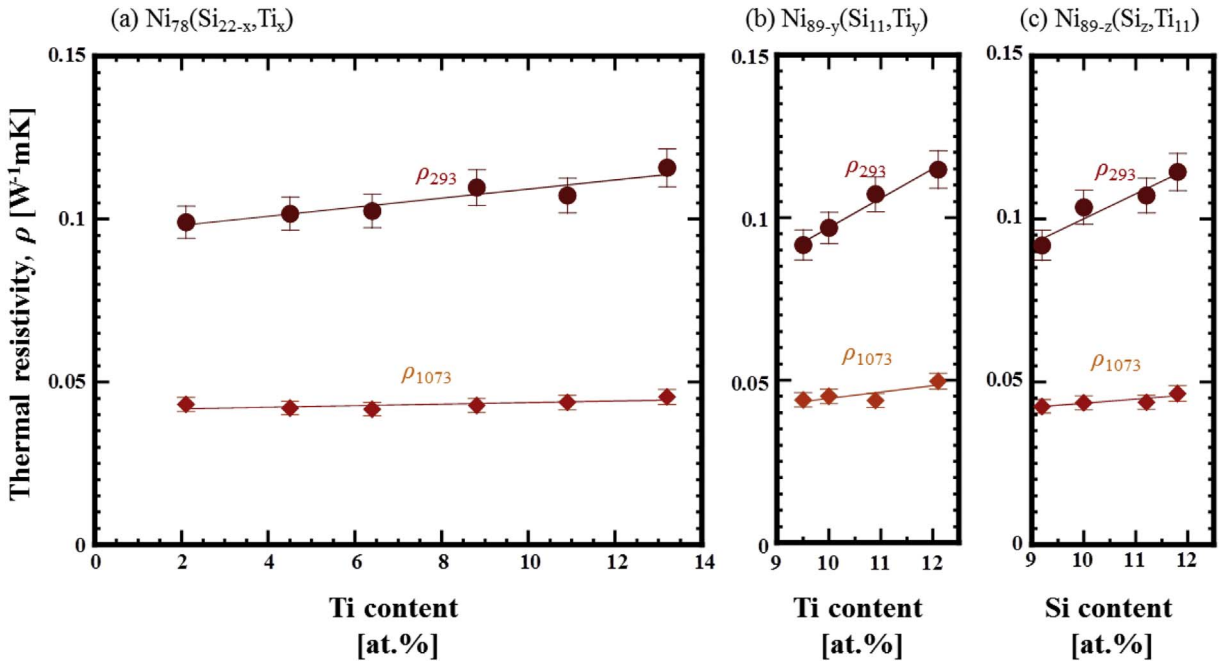

Fig. 8. Variations of the thermal resistivity at 293 K and 1073 K of the (a) $Ni_{78}(Si_{22-x},Ti_x)$, (b) $Ni_{89-y}(Si_{11},Ti_y)$, and (c) $Ni_{89-z}(Si_z,Ti_{11})$ alloys as a function of the elemental content.

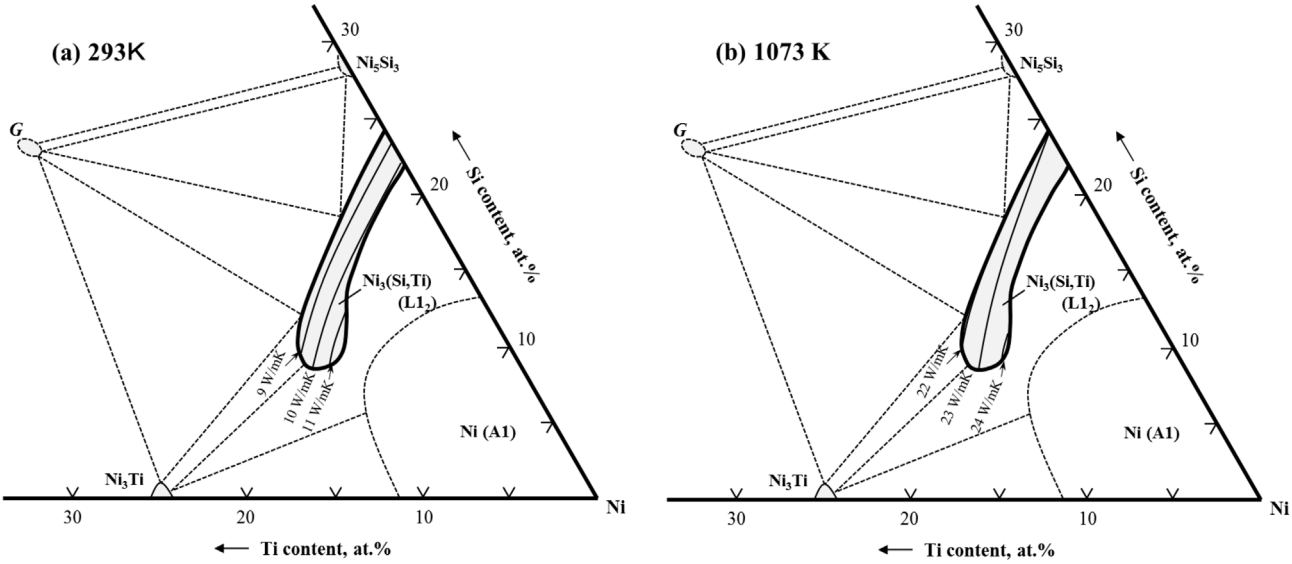

Fig. 9. Contour map of the thermal conductivity at (a) 293 K and (b) 1073 K for the $Ni_3(Si,Ti)$ single-phase specimens, which were drawn in the partial phase diagram of Ni-Si-Ti ternary system.

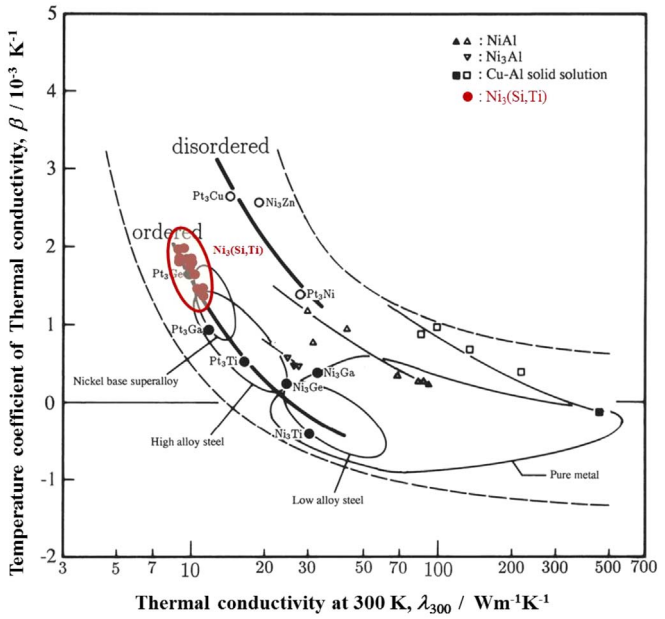

Fig. 10. Relationship between thermal conductivity at 300 K and temperature coefficient for various metallic systems reported by Terada et al. [15]. The data for $Ni_3(Si,Ti)$ single-phase alloys obtained in this study were plotted as red solid circles. (For interpretation of the references to colour in this figure legend, the reader is referred to the web version of this article.)

steels and nickel alloys with a low thermal conductivity at 300 K exhibit a positive coefficient. In the case of Ni_3X and Pt_3X compounds, the inverse correlation is held and can be classified into either ordered intermetallic compounds or disordered alloys as indicated by the two thick solid lines in Fig. 10.

The temperature coefficient of thermal conductivity, β, of the $Ni_3(Si,Ti)$ single-phase specimens was converted from the temperature coefficient, α, calculated by eq. (2), and then plotted using solid circles in Fig. 10. This confirmed that β for the $Ni_3(Si,Ti)$ single-phase specimens was located near the curve for the ordered intermetallic compounds. The $Ni_3(Si,Ti)$ single-phase alloys have a relatively higher β than the other ordered intermetallic compounds, such as Ni_3Ga, Ni_3Ge, and Pt_3Ti, because they have a relatively lower thermal conductivity at room temperature. This suggests that the thermal conductivity of the $Ni_3(Si,Ti)$ single-phase alloys at high temperatures above 1073 K approach that of the compounds Ni_3Ga, Ni_3Ge, and Pt_3Ti, although the thermal conductivity at 300 K is low. This is favorable for high-temperature applications.

5. Summary

The effects of composition and temperature on the thermal conductivity at temperatures ranging from 293 K to 1073 K were investigated for $Ni_3(Si,Ti)$ single-phase alloys. The microstructure of the alloys with a nominal composition of $Ni_{78}(Si_{22-x},Ti_x)$ (x = 2 to 12 at.%), $Ni_{89-y}(Si_{11},Ti_{11-y})$ (y = 9.5 to 12 at.%), and $Ni_{89-z}(Si_z,Ti_{11})$ (z = 9.5 to 12 at.%) was identified as single-phase $Ni_3(Si,Ti)$ with an $L1_2$ structure. The thermal conductivity at 293 K, λ_{293}, of the single-phase alloys was found to range from 8 W/mK to 12 W/mK, which is lower than that of other alloys with an ordered $L1_2$ structure such as Ni_3Al and Ni_3Ga. The observed increase in λ_{293} was more sensitive toward the increase in the Ni content than toward the Si and Ti content. The thermal conductivity of the $Ni_3(Si,Ti)$ single-phase alloys increased monotonically with increasing temperature, which should be more significant than the other ordered alloys with an $L1_2$ structure, and follows Mooij's relationship. Since the temperature coefficient of thermal conductivity tends to increase because of the low value of λ_{293}, the compositional dependency of the $Ni_3(Si,Ti)$ single-phase alloys becomes less significant at higher temperatures.

Funding

Financial support provided by the Japan Society for the Promotion of Science (JSPS) as a Grant-in-Aid for Scientific Research (C) (No. 26420663) is gratefully acknowledged.

Acknowledgements

The authors are grateful to Prof. N. Masahashi of the Institute for Materials Research (IMR) at Tohoku University for useful discussions and comments. The authors also thank Dr. M. Ishikuro, Mr. E. Aoyagi, and Mr. S. Itoh of the IMR for their technical assistance.

References

[1] D.P. Pope, S.S. Ezz, Mechanical properties of Ni_3Al and nickel-based alloys with

high volume fraction of γ', Int. Mater. Rev. 29 (1984) 136–167.
[2] N.S. Stoloff, Physical and mechanical metallurgy of Ni_3Al and its alloys, Int. Mater. Rev. 34 (1989) 153–184.
[3] M. Yamaguchi, Y. Umakoshi, The deformation behavior of intermetallic superlattice compounds, Prog. Mater. Sci. 34 (1990) 1–148.
[4] K.S. Kumar, J.H. Westbrook, R.L. Fleischer (Eds.), Intermetallic Compounds, John Wiley & Sons, 1995, pp. 211–235.
[5] S.C. Deevi, V.K. Sikka, C.T. Liu, Processing, properties, and applications of nickel and iron aluminides, Prog. Mater. Sci. 42 (1997) 177–192.
[6] Y. Umakoshi, K. Hagihara, T. Nakano, Operative slip systems and anomalous strengthening in Ni_3Nb single crystals with the $D0_a$ structure, Intermetallics 9 (2001) 955–961.
[7] M. Yamaguchi, H. Inui, K. Ito, High-temperature structural intermetallics, Acta Mater. 48 (2000) 307–322.
[8] T. Takasugi, D. Shindo, O. Izumi, M. Hirabayashi, Metallographic and structural observations in the pseudo-binary section Ni_3Si-Ni_3Ti of the $Ni-Si-Ti$ system, Acta Metall. Mater. 38 (1990) 739–745.
[9] T. Takasugi, M. Nagashima, O. Izumi, Strengthening and ductilization of Ni_3Si by addition of Ti elements, Acta Metall. Mater. 38 (1990) 747–755.
[10] T. Takasugi, O. Izumi, M. Yoshida, Mechanical properties of recrystallized $L1_2$-type $Ni_3(Si,Ti)$ alloys, J. Mater. Sci. 26 (1991) 1173–1178.
[11] Y. Kaneno, I. Nakaaki, T. Takasugi, Texture evolution during cold rolling and recrystallization of $L1_2$-type ordered $Ni_3(Si,Ti)$, Intermetallics 10 (2002) 693–700.
[12] Y. Kaneno, T. Myoki, T. Takasugi, Tensile properties of $L1_2$ intermetallic foils fabricated by cold rolling, Int. J. Mater. Res. 99 (2008) 1229–1236.
[13] D. Imajo, Y. Kaneno, T. Takasugi, Effect of Ta substitution method on the mechanical properties of $Ni_3(Si,Ti)$ intermetallic alloy, Mater. Sci. Eng. A 588 (2013) 228–238.
[14] A. Hashimoto, Y. Kaneno, S. Semboshi, T. Takasugi, Anomalous hardening behavior accompanied by reordering of plastically deformed $Ni_3(Si,Ti)$ intermetallic alloy, Mater. Sci. Eng. A 610 (2014) 228–236.
[15] Y. Terada, K. Ohkubo, T. Mohri, T. Suzuki, Thermal conductivity of Ni_3X and Pt_3X in ordered and disordered states, Mater. Sci. Eng. A 239–240 (1997) 907–914.
[16] Y. Terada, K. Ohkubo, K. Nakagawa, T. Mohri, T. Suzuki, Thermal conductivity of B2-type aluminides and titanides, Intermetallics 3 (1995) 347–355.
[17] W.J. Parker, R.J. Jenkins, C.P. Butler, G.L. Abbott, Flash method of determining thermal diffusivity, heat capacity and thermal conductivity, J. Appl. Phys. 32 (1961) 1679–1684.
[18] S. Min, J. Blumm, A. Lindemann, A new laser flash system for measurement of the thermophysical properties, Thermochim. Acta 455 (2007) 46–49.
[19] T.G. Santos, P. Vilaca, R.M. Miranda, Electrical conductivity field analysis for evaluation of FSW joints in AA3013 and AA7075 alloys, J. Mater. Proc. Tech. 211 (2011) 174–180.
[20] X. Zheng, D.G. Cahill, P. Krasnochtchekov, R.S. Averback, J.C. Zhao, High-throughput thermal conductivity measurement of nickel solid solutions and the applicability of the Wiedemann-Franz law, Acta Mater. 55 (2007) 5177–5188.
[21] D.R. Poirier, E. McBride, Thermal conductivities of hypoeutectic Al-Cu alloys during solidification and cooling, Mater. Sci. Eng. A 224 (1997) 48–52.
[22] Y. Oya, T. Suzuki, Nickel-rich portion of the Ni-Si phase diagram, Z. Met. 74 (1983) 21–24.
[23] Y. Terada, K. Ohkubo, K. Nakagawa, T. Mohri, T. Suzuki, Thermal conductivity of Ni_3Al with ternary additions, Mater. Sci. Eng. A 311 (2001) 232–235.
[24] Y. Terada, K. Ohkubo, T. Mohri, T. Suzuki, Thermal conductivity of Intermetallic compounds with metallic bonding, Mater. Trans. 12 (2002) 3167–3176.
[25] S. Semboshi, H. Tsuda, Y. Kaneno, A. Iwase, T. Takasugi, Thermal conductivity of Ni_3Al-Ni_3V pseudo-binary alloys, Intermetallics 59 (2015) 1–7.
[26] J. Miyake, M.E. Fine, Electrical conductivity versus strength in a precipitation hardened alloy, Acta Metall. Mater. 40 (1992) 733–741.
[27] C. Wei, N. Antolin, O.D. Restrepo, W. Windl, J.-C. Zhao, A general model for thermal and electrical conductivity of binary metallic systems, Acta Mater. 126 (2017) 272–279.
[28] Y. Terada, K. Ohkubo, T. Mohri, T. Suzuki, Thermal conductivity in nickel solid solutions, J. Appl. Phys. 81 (1997) 2263–2268.
[29] J.H. Mooij, Electrical conduction in concentrated disordered transition metal alloys, Phys. Status Solidi A 17 (1973) 521.
[30] Y. Shirai, K. Masaki, T. Inoue, S.R. Nishitani, M. Yamaguchi, Electrical resistivity of L12 trialuminides containing 3d transition element, Intermetallics 3 (1995) 381.